Research in Astron. Astrophys. **2010** Vol. **10** No. **1**, 96 – 106
http://www.raa-journal.org *http://www.iop.org/journals/raa*

Research in Astronomy and Astrophysics

Nonlinear adaptive observer-based sliding mode control for LAMOST mount driving *

Wang-Ping Zhou[1], Yi Zheng[2], Wei Guo[1], Li Yu[1] and Chang-Song Yang[1]

[1] School of Information & Control Engineering, Nanjing University of Information Science & Technology, Nanjing 210044, China; *wpzhou@yahoo.cn*

[2] Nanjing Institute of Astronomical Optics & Technology, National Astronomical Observatories, Chinese Academy of Sciences, Nanjing 210042, China

Received 2009 March 23; accepted 2009 September 27

Abstract Heavy disturbances caused mainly by wind and friction in the mount drive system greatly impair the pointing accuracy of the Large Sky Area Multi-Object Fiber Spectroscopic Telescope (LAMOST). To overcome this negative effect, a third order Higher Order Sliding Mode (HOSM) controller is proposed. The key part of this approach is to design an appropriate observer which obtains the acceleration state. A nonlinear adaptive observer is proposed in which a novel polynomial model is applied to estimate the internal disturbances of the mount drive system. Theoretical analysis demonstrates the stability of the proposed observer. Simulation results show that this nonlinear adaptive observer can obtain a high precision acceleration signal which completes the HOSM controller. Furthermore, the HOSM approach can easily satisfy the position tracking requirements of the LAMOST mount drive system.

Key words: methods: analytical — methods: numerical — methods: laboratory — telescopes

1 INTRODUCTION

With the development of astrophysics, larger aperture telescopes are greatly needed. This is where the LAMOST telescope comes from. However, large telescopes, like LAMOST, all confront a common technical challenge–how to obtain high pointing accuracy when the mechanical structure of the mount drive system becomes bigger and bigger. Two factors that seriously affect the performance of the mount drive system are wind buffeting and uncertainties inside the system. The mount itself is a massive reflecting mirror with a 6 m diameter, which is supported by a giant mechanism. During astronomical observations, the mirror needs to be driven on two vertical axes and exposed to the open air to receive starlight (Xu 2000). Thus, it is very likely that stability in the motion of the mount will suffer from wind buffeting. As for the internal uncertainties, the fluctuation of friction torque is the main issue that should be addressed. Nowadays, the so-called friction drive is frequently utilized in mount drive systems of contemporary astronomical telescopes, and the LAMOST telescope is no exception. The main advantage of a friction drive is to achieve high positioning accuracy without the nuisance of backlash which exists in many conventional gear drive systems. However, since friction

* Supported by the National Natural Science Foundation of China.

drive itself is a complex nonlinear process, it may lead to torque fluctuation that affects the tracking performance. Thus, the problem is how to deal with these nonlinear disturbances and get more accurate control.

A detailed control strategy in dealing with these nonlinear disturbances has not been well studied in most telescope mount drive systems. A commonly used method that counteracts the disturbances in the mount drive system is Proportional-Integral-Derivative (PID) and its transformations. The combined PI and P controllers may be found in the Keck mount drive system, i.e. a Proportional-Integral controller in the position loop and a Proportional controller in the velocity loop (Sirota & Thompson 1994). Dupont (1994) has studied a Proportional-Derivative controller to restrain the stick-slip phenomenon caused by internal nonlinear friction torque. Although the PID approach can totally remove the effect of the step disturbance signal, it has a steady error approximating the reciprocal of proportional gain when the disturbance is a slope signal (Xu & Yan 2004). The pole displacement control used in the mount drive system of the Gemini telescope takes the main disturbances as part of the identified system model, while the control performance may be decreased by new disturbances (Burns 1994). Medrano-Cerda et al. (2002) have studied an H-infinity controller for the mount drive of a 2 m telescope. With the physical plant being considered as a system cluster, the H-infinity approach uses analytical forms to design the controller, which makes any plant in the system cluster meet the desired control performance. This approach may obtain high precision control in the mount drive of large telescopes (Erm et al. 2004; Zhou et al. 2006). Nevertheless, the dynamic response is relatively slow.

Since the task of the control system with a friction drive involves ultra-low speed motions, nonlinear disturbances will be significant in the dynamics and nonlinear control may be necessary to achieve the desired performance. Nowadays, nonlinear controllers like backstepping (Hirvonen et al. 2006) and sliding mode (Bartolini et al. 2003) controllers are becoming more popular due to the development of design methods and computer science. The most obvious way to withstand the uncertainties in the disturbances is to keep some constraints by sufficient force, which immediately corrects any deviation of the system from the constraints. Implemented directly, the approach leads to the so-called sliding mode (Perruquetti & Barbot 2002). Having proved its high accuracy and robustness with respect to various internal and external disturbances, it also reveals its main drawback: the so-called chattering effect. To avoid chattering, some approaches have been described in the literature (Feng & Fei 1998). The main idea is to change the dynamics in some small vicinity of the discontinuous surface in order to avoid real discontinuity and, at the same time, preserve the main properties of the whole system. However, the ultimate accuracy and robustness of the sliding mode are partially lost (Furuta & Pan 2000).

The newly developed higher order sliding mode (HOSM) generalizes the basic sliding mode idea. It acts on the higher order time derivatives of the system deviation from the constraint while the influenced counterpart is of first order in the standard sliding mode. Along with keeping the main advantages of the original approach, at the same time, it totally removes the chattering effect and provides for even higher accuracy in its implementation (Perruquetti & Barbot 2002). A new nonlinear adaptive observer based on Marino & Tomei (2006) is proposed, where a polynomial made up of the lower power of the output state is used for adaptively approximating the nonlinear disturbances. In this study, a so-called nonlinear adaptive observer is designed to obtain the acceleration state, which completes a higher third order sliding mode controller.

2 PROBLEM STATEMENT

In the case of LAMOST, the mount is driven on two vertical axes, i.e. the azimuth transmission and altitude transmission. These two motions are dynamically independent yet have the same major configuration characterization. Hence, it is sufficient to study one of them while the resulting con-

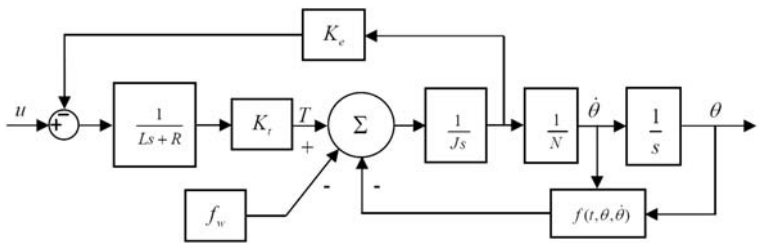

Fig. 1 Block diagram of the mount driven servo system.

clusions may apply to the other in the same way. Here, azimuth axis motion is chosen for analysis at the preliminary research stage.

Figure 1 shows a block diagram of LAMOST's azimuth axis drive transfer functions, where s represents the Laplacian, u denotes drive voltage, L and R are armature inductance and resistance of the drive motor respectively, K_{t} is the torque coefficient of the drive motor, K_{e} denotes the motor's counter electromotive force coefficient, T is the initial torque generated by the motor, J is the moment of inertia that is converted to the motor axis, N is the angular velocity ratio between the motor and the driven wheel, $\dot{\theta}$ and θ denote the driven wheel's angular velocity and displacement respectively, f_{w} denotes the external disturbances (wind buffeting in particular), and $f(t, \theta, \dot{\theta})$ describes uncertainties inside the system. In order to achieve drive performance with high precision, it is essential to first study the properties of wind and internal uncertainties. According to Zhou et al. (2006), a detailed description of wind buffeting and internal uncertainties is given as follows.

2.1 Wind Buffeting

The mount of LAMOST carries the reflecting Schmidt plate, which consists of 24 pieces of hexagonal sub-mirrors with a total diameter of about 6 m. The telescope structure is erected on Xinglong Mountain about 1000 m above sea level. The local environment features seasonal high winds, which provoke huge disturbances that might generate wind vibration and deteriorate the performance of the mount movement. To control wind disturbance, it is first necessary to find a wind model that can predict the disturbance. A commonly used wind model is the Davenport spectral density model, which separates the torque of wind disturbance into two parts (Davenport 1995): one is the time-invariant part, which brings a constant torque; the other is the time-varying part. The constant part can be described by

$$T_{\mathrm{const}} = C_{\mathrm{T}} q A D, \tag{1}$$

where C_{T} is the wind torque coefficient, $q = 1/2\rho V^2$ denotes the dynamic pressure, ρ is the density of air, V denotes mean horizontal wind velocity, A represents the contact area and D is the radius of the axis which is vertical to A. Because the period of the wind's time-varying part is very short, from further calculation, the torque of the time-varying part can be simplified as follows

$$T_{\mathrm{vary}} = \rho C_L A V v(t), \tag{2}$$

where C_L is the mean wind pressure coefficient, $v(t)$ denotes the oscillating horizontal wind velocity with respect to the shaft. In Equation (2), all the coefficients except $v(t)$ are constant. Therefore, it is reasonable to use a random quantity to simulate the disturbance torque caused by wind.

2.2 Internal Uncertainties

With respect to the internal uncertainties, the variable load torque caused by the friction drive will be the dominant factor. The friction mechanism applied in the main axes structure of astronomical telescopes can generally be simplified as a pair of wheels in contact along a common cylindrical generatrix. One wheel in the pair is the driving wheel and the other is the driven wheel with radially applied force supplying a close contact between the two wheels. The friction in the contact area between the driving wheel and the driven wheel features complex motions such as pre-sliding displacement, break-away, and stick-slip, etc., thus making friction an important aspect of high quality servo systems. Model-based friction compensation schemes resort to a suitable friction model to predict the friction without adopting high gain control loops. The representative LuGre friction model has been applied to many friction compensation control systems. It is derived from the bristle model assuming that the friction interface is thought of as a contact between bristles. By introducing a nonlinear internal friction state, the friction force can be described by (Canudas De Wit 1998)

$$\begin{aligned} F &= \sigma_0 z + \sigma_1 \dot{z} + \sigma_2 \dot{\theta}, \\ \dot{z} &= \dot{\theta} - (|\dot{\theta}|/g(\dot{\theta}))z, \\ \sigma_0 g(\dot{\theta}) &= F_{\mathrm{C}} + (F_{\mathrm{S}} - F_{\mathrm{C}})e^{-(\dot{\theta}/\dot{\theta}_{\mathrm{S}})^2}, \end{aligned} \tag{3}$$

where z and θ are the internal states of the friction model and the position of the system respectively, σ_0 and σ_1 are terms of the bristle model, σ_2 is the viscous friction coefficient, F_{C} and F_{S} represent Coulomb friction and static friction respectively, $\dot{\theta}_{\mathrm{S}}$ denotes the Streibeck velocity, and $\sigma_0 g(\dot{\theta})$ describes the Streibeck behavior. Figure 2 shows the friction torque against the corresponding velocity by simulation in a Matlab language, which approximately reflects the nonlinearity of internal uncertainties in the mount drive system.

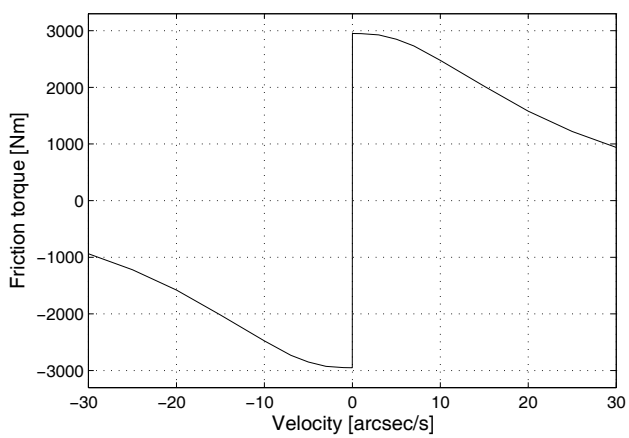

Fig. 2 Simulation of friction torque against velocity.

2.3 System Differential Equation Description

In Figure 1, f_{w} is used to describe the nonlinear external disturbances, specifically wind buffeting; at the same time, $f(t, \theta, \dot{\theta})$ and an additional term $\Delta(t, \theta, \dot{\theta})$ (which considers the unmodeled dynamics between the actual system and the model) calculates the uncertainties inside the system. Letting

$x_1 = \theta$, $x_2 = \dot{\theta}$, and $x_3 = T$, the LAMOST main axes servo system state space differential equation description has the form

$$\begin{aligned} \dot{x_1} &= x_2, \\ \dot{x_2} &= \frac{1}{JN}x_3 - \frac{1}{JN}[f_{\mathrm{w}} + f(t, x_1, x_2)], \\ \dot{x_3} &= -\frac{R}{L}x_3 - \frac{NK_{\mathrm{e}}K_{\mathrm{t}}}{L}x_2 + \frac{K_{\mathrm{t}}}{L}u. \end{aligned} \tag{4}$$

Note that, in Equation (4), $f(t, x_1, x_2) = f(t, \theta, \dot{\theta}) + \Delta(t, \theta, \dot{\theta})$. It is easy to form a conventional sliding mode control with the above mentioned system state space differential equation. To do this, an error system will first be defined. Letting $k(t)$ denote the tracking reference signal, $e_1 = x_1 - k(t)$, $e_2 = x_2 - \dot{k}(t)$, and $e_3 = \frac{1}{JN}x_3 - \frac{1}{JN}[f_{\mathrm{w}} + f(t, x_1, x_2)] - \ddot{k}(t)$, then the error system differential equation can be written in the form

$$\begin{aligned} \dot{e_1} &= e_2, \\ \dot{e_2} &= e_3, \\ \dot{e_3} &= -\frac{NK_{\mathrm{e}}K_{\mathrm{t}}}{JNL}x_2 - \frac{R}{JNL}x_3 - \frac{1}{JN}[\dot{f}_{\mathrm{w}} + \dot{f}(t, x_1, x_2)] - \ddot{k}(t) + \frac{K_{\mathrm{t}}}{JNL}u. \end{aligned} \tag{5}$$

Based on the differential Equations (4) and (5), a higher third order sliding mode controller is designed for LAMOST's main axes in the subsequent section.

3 HIGHER ORDER SLIDING MODES CONTROL

The basic control idea of HOSM is actually movement of a discontinuous set of dynamic systems understood in the Filippov sense (Levant 1998), and the sliding order characterizes the degree of smoothness in the dynamics in the vicinity of the mode. If s is a smooth function and the task is to keep a constraint defined by $s = 0$, the sliding order is the number of continuous total derivatives of s (including the zero one) in the vicinity of the sliding mode. Therefore, the rth order sliding mode is determined by

$$s = \dot{s} = \ddot{s} = \ldots = s^{(r-1)} = 0, \tag{6}$$

forming an r-dimensional condition on the state of the dynamic system. The standard sliding mode, on which most variable structure systems are based, is of first order ($\dot{s}$ is discontinuous). While the standard modes feature finite time convergence, convergence to HOSM may be asymptotic as well.

To develop the general procedures for a nonlinear plant, one may first use a diffeomorphism to obtain a canonical representation of the plant dynamics. Assuming that there exists a diffeomorphism that could change the dynamics of our servo system into an affine nonlinear system with the form

$$\dot{x} = \alpha(t, x) + \beta(t, x)u, \qquad s = s(t, x) \tag{7}$$

where $x \in \mathbf{R}^n$, $u \in \mathbf{R}$, and α, β and s are smooth functions. If the system has a relative degree r, the control signal first appears in the rth full time derivative of s with $\frac{ds^{(r)}}{du} \neq 0$ and the Lie derivatives $L_\alpha s = L_\beta L_\alpha s =, \ldots, = L_\beta L_\alpha^{(r-2)} s = 0$ in the vicinity of the given point. The control task is to constrain the system dynamics exactly on the manifold $s(t, x) = 0$ through discrete switching. The relevant motions correspond to an rth sliding mode for s, $\dot{s}$,..., $s^{(r-1)}$ are continuous functions with respect to t and x.

Let $y_1 = s$, $y_2 = \dot{s}$,..., $y_r = s^{(r-1)}$. Under these above assumptions, we have

$$\begin{aligned} \dot{y}_1 &= y_2, \quad \dot{y}_2 = y_3, \quad \ldots \\ \dot{y}_{r-1} &= y_r, \quad \dot{y}_r = L_\alpha^r s + L_\beta L_\alpha^{r-1} u. \end{aligned} \tag{8}$$

For the general nonlinear problem, one may choose an equivalent control $u_{\mathrm{eq}} = \frac{-L_\alpha^r}{L_\beta L_\alpha^{r-1} s}$ to meet the control requirement. In ordinary sliding mode control, we can choose $u = -K\ \mathrm{sign}(s)$, where K is a constant, the value of which is greater than the upper bound of the absolute value of u_{eq}. The solution of the corresponding differential equation is the rth sliding mode when we substitute $u = u_{\mathrm{eq}}$ into Equation (7). However, such a mode is usually unstable because $L_\beta L_\alpha^{r-1} s = \frac{d}{du} s^{(r)}$, and $h = L_\alpha^r s$ is the time total derivative of s when $u = 0$. So, the problem is transformed into finding a discrete feedback $u = U(t, x)$ to constrain the system dynamics on the rth sliding mode.

Defining

$$s = e_1 = x_1 - k(t) = 0,$$

$$\alpha(t, x) = x_2 \frac{\partial}{\partial x_1} + \frac{1}{JN}[x_3 - f(t, x_1, x_2)] \frac{\partial}{\partial x_2} + \frac{1}{L}(-NK_{\mathrm{e}}K_{\mathrm{t}}x_2 - Rx_3) \frac{\partial}{\partial x_3},$$

$$\beta(x) = K_{\mathrm{t}}/L \frac{\partial}{\partial x_3}, \tag{9}$$

we get

$$L_\beta s = 0, L_\beta L_\alpha s = 0, L_\beta L_\alpha^2 s \neq 0. \tag{10}$$

It is trivial that there is a third order sliding mode relative degree in the system Equation (4). From further calculation, we can find some positive numbers K_m, K_M and C, which satisfy

$$0 < K_m \leq \frac{\partial}{\partial u} s^{(r)} \leq K_M, \quad |L_\alpha^r s| \leq C. \tag{11}$$

According to Levant (2003), the high third order sliding mode controller for the drive system is given by

$$u = -a\mathrm{sign}(\ddot{s} + 2(|\dot{s}|^3 + |s|^2)^{\frac{1}{6}} \mathrm{sign}(\dot{s} + |s|^{\frac{2}{3}} \mathrm{sign}(s)), \tag{12}$$

where a is a positive number denoting the motor control voltage and the sign is a symbolic function. In practical implementations, the velocity and position are measurable signals such that s and $\dot{s}$ are obtained. The only unknown signal is acceleration which is concealed in $\ddot{s}$ in controller Equation (12).

4 DESIGN OF THE NONLINEAR ADAPTIVE OBSERVER

The major problem of designing an observer has to do with those unknown nonlinear uncertainties f_w and $f(t, x_1, x_2)$. A commonly used approach to cope with a nonlinear function is linearization at some given point. Although the uncertainties cannot be modeled exactly, just like in the linearization process, they may be approximated by a combination of lower order items. Letting k be a constant, a parameterized model for the uncertainties may be given by

$$f_w + f(t, x1, x2) \approx \beta(t, x)\vartheta = [k \ \ kx_1 \ \ kx_2 \ \ x_1x_2 \ \ x_1^2 \ \ x_2^2]\vartheta, \tag{13}$$

where $\vartheta^T = [\vartheta_1, ..., \vartheta_6]$, $\beta(t, x) = [k \ \ kx_1 \ \ kx_2 \ \ x_1x_2 \ \ x_1^2 \ \ x_2^2]$. Apparently, ϑ is the optimal parameter for estimating uncertainties f_w and $f(t, x_1, x_2)$. If some $\hat{\vartheta}$ is found with an appropriate adaptive law that best approximates ϑ, then the nonlinear adaptive observer could be used to estimate the acceleration signal. The following is the design process of the nonlinear adaptive observer.

Given some shorthand, $a_1 = \frac{1}{JN}$, $a_2 = -\frac{NK_{\mathrm{e}}K_{\mathrm{t}}}{L}$, $a_3 = -\frac{R}{L}$, and $g = \frac{K_{\mathrm{t}}}{L}$, Equation (4) may be rewritten in the form

$$\dot{x} = f(x) + g(x, u) + \sum_{i=1}^{p} \vartheta_i q_i(x, u),$$

$$y = h(x), \tag{14}$$

where $f(x) = x_2\frac{\partial}{\partial x_1} + a_1x_3\frac{\partial}{\partial x_2} + (a_2x_2 + a_3x_3)\frac{\partial}{\partial x_3}$, $g(x,u) = g\frac{\partial}{\partial x_3}$, and $q(x,u) = -\frac{1}{JN}\beta(t,x)\vartheta\frac{\partial}{\partial x_2}$. Based on Marino & Tomei (2006), it is easy to find a global diffeomorphism

$$T = \begin{bmatrix} -a_1a_2x_1 - a_3x_2 + a_1x_3 \\ -a_3x_1 + x_2 \\ x_1 \end{bmatrix}, \tag{15}$$

which transforms system Equation (14) into the following

$$\dot{z} = \underbrace{\begin{bmatrix} 0 & 0 & 0 \\ 1 & 0 & 0 \\ 0 & 1 & 0 \end{bmatrix}}_{=A_0} z + \begin{bmatrix} a_1gu \\ a_1a_2y \\ a_3y \end{bmatrix} + \begin{bmatrix} \frac{a_3}{JN}\beta(t,y,u)\vartheta \\ -\frac{1}{JN}\beta(t,y,u)\vartheta \\ 0 \end{bmatrix},$$

$$y = c_0z = z_3, \tag{16}$$

where $z = [z_1 \quad z_2 \quad z_3]^T$ denotes the new state variable, y is the output of the system, $c_0 = [0 \quad 0 \quad 1]$.

Assume that all zeros of the polynomial $x^2 + b_2x + b_1$ have negative real parts, where x denotes an unknown variable, and $b = [b_1 \quad b_2 \quad 1]^T$ is some positive vector. A transform filter is defined by

$$\eta_1 = z_1 - \xi_1\vartheta, \quad \eta_2 = z_2 - \xi_2\vartheta, \quad \eta_3 = z_3, \tag{17}$$

where the dynamic equation of ξ is

$$\dot{\xi} = \begin{bmatrix} 0 & -b_1 \\ 1 & -b_2 \end{bmatrix}\xi + \begin{bmatrix} 1 & 0 & -b_1 \\ 0 & 1 & -b_2 \end{bmatrix}\begin{bmatrix} \frac{a_3}{JN}\beta(t,y,u)\vartheta \\ -\frac{1}{JN}\beta(t,y,u)\vartheta \\ 0 \end{bmatrix},$$

i.e.

$$\dot{\xi}_1 = -b_1\xi_2 + \frac{a_3}{JN}\beta(t,y,u)\vartheta, \qquad \dot{\xi}_2 = \xi_1 - b_2\xi_2 - \frac{1}{JN}\beta(t,y,u)\vartheta,$$

so we get

$$\dot{\eta}_1 = \dot{z}_1 - \dot{\xi}_1\vartheta = a_1gu + b_1\xi_2\vartheta,$$

$$\dot{\eta}_2 = \dot{z}_2 - \dot{\xi}_2\vartheta = z_1 + a_1a_2y - \xi_1 + b_2\xi_2\vartheta = \eta_1 + a_1a_2y + b_2\xi_2\vartheta,$$

$$\dot{\eta}_3 = \dot{z}_3 = z_2 + a_3y - \xi_2\vartheta + \xi_2\vartheta = \eta_2 + \xi_2\vartheta. \tag{18}$$

The filter (17) transforms system (16) into an observable normative form:

$$\dot{\eta} = \underbrace{\begin{bmatrix} 0 & 0 & 0 \\ 1 & 0 & 0 \\ 0 & 1 & 0 \end{bmatrix}}_{=A_0} \eta + \begin{bmatrix} a_1gu \\ a_1a_2y \\ a_3y \end{bmatrix} + \begin{bmatrix} b_1 \\ b_2 \\ 1 \end{bmatrix}\xi_2\vartheta,$$

$$y = c_0\eta = \eta_3. \tag{19}$$

THEOREM: Let λ be an arbitrary positive number, $k = -(A_0b + \lambda b)$, and Γ be an arbitrary positive definite symmetrical matrix. The system with normative form (19) has an adaptive observer as follows

$$\dot{\hat{\eta}} = \underbrace{\begin{bmatrix} 0 & 0 & -\lambda b_1 \\ 1 & 0 & -(b_1 + \lambda b_2) \\ 0 & 1 & -(b_2 + \lambda) \end{bmatrix}}_{=A} \hat{\eta} + \begin{bmatrix} a_1gu \\ a_1a_2y \\ a_3y \end{bmatrix} + \begin{bmatrix} b_1 \\ b_2 \\ 1 \end{bmatrix}\xi_2\hat{\vartheta} - ky,$$

$$\dot{\hat{\vartheta}} = \Gamma\xi_2(y - c_0\hat{\eta}). \tag{20}$$

Proof: Defining $\tilde{\eta} = \eta - \hat{\eta}$, $\tilde{\vartheta} = \vartheta - \hat{\vartheta}$, we can write the error equation of the observer

$$\dot{\tilde{\eta}} = \underbrace{\begin{bmatrix} 0 & 0 & -\lambda b_1 \\ 1 & 0 & -(b_1 + \lambda b_2) \\ 0 & 1 & -(b_2 + \lambda) \end{bmatrix}}_{=A} \tilde{\eta} + b\xi_2 \tilde{\vartheta},$$

$$\dot{\tilde{\vartheta}} = -\Gamma \xi_2^T c_0 \tilde{\eta}. \tag{21}$$

Because all zeros of the polynomial based on b have negative real parts, each eigenvalue of matrix A may be characterized as being the same. Hence, the Lyapunov matrix equation $A^T P + PA = -Q$ has only one symmetric positive definite solution P with respect to the symmetric positive definite matrix Q, where $Pb = c_0^T$.

Let a Lyapunov candidate be

$$V = \tilde{\eta}^T P \tilde{\eta} + \tilde{\vartheta}^T \Gamma^{-1} \tilde{\vartheta}.$$

Differentiating both sides of the above equation with respect to time, we obtain that

$$\begin{aligned} \dot{V} &= (A\tilde{\eta} + b\xi_2\tilde{\vartheta})^T P\tilde{\eta} + \tilde{\eta}^T P(A\tilde{\eta} + b\xi_2\tilde{\vartheta}) + (-\Gamma\xi_2^T c_0\tilde{\eta})^T \Gamma^{-1}\tilde{\vartheta} + \tilde{\vartheta}^T\Gamma^{-1}(-\Gamma\xi_2^T c_0\tilde{\eta}) \\ &= \tilde{\eta}^T(A^T P + PA)\tilde{\eta} = -\tilde{\eta}^T Q\tilde{\eta}. \end{aligned}$$

The positive definite Q satisfies $\dot{V} < 0$ which guarantees uniform stability around origin $(\tilde{\eta}, \tilde{\vartheta}) = 0$. Therefore, the correctness of the given adaptive observer described by Equation (20) is transparent and the acceleration signal $\ddot{\theta}$ could be found with the form

$$\ddot{\theta} = \hat{\eta}_1 + a_3\hat{\eta}_2 + ((a_3 + \lambda)b_2 + a_3\lambda + b_1)(y - \hat{\eta}_3) + (a_3^2 + a_1 a_2)y + (a_3\xi_2 + \xi_1 - \frac{1}{J_{\mathrm{eq}}N}\Delta)\hat{\vartheta}. \tag{22}$$

5 SIMULATION EXPERIMENT

The detailed parameters of the LAMOST main axis and drive motors may be found in our earlier research (Zhou & Xu 2008). In this study, we will continue to use them. Based on subsections 2.1 and 2.2, we found simulation models of external and internal nonlinear disturbances to approximate the practical disturbances in the real drive system. From calculation, the maximum disturbance torque caused by wind under 10 m per second is about 300 Nm, so we add random numbers between –300 and +300 to simulate wind disturbance.

The typical sine wave and slope signals are chosen as the expected position references to test the tracking performance of the proposed adaptive observer based HOSM position control. One is $10'' \sin t + 10''$, and the other is $1''t + 1''$ ($1'' = 1$ arcsec$= 4.81 \times 10^{-6}$ radian). Figure 3 shows the observed disturbances vs. the real disturbances when position tracking these two signals respectively. It is obvious that the proposed nonlinear adaptive observer can exactly capture the real disturbances in the system. Figure 4 shows the observed acceleration signals of the two typical references respectively. One can clearly see from the figure that the observed signals are constrained in a very small vicinity of the references as time goes by. Therefore, it is sufficient to use the adaptive observer to estimate the required acceleration signals in HOSM control.

The tracking performance of the third order sliding mode controller based on the proposed nonlinear adaptive observer is shown in Figures 5 and 6 with a given sine wave reference signal. In order to simulate real situations, noise is added to both the position and velocity measurements. It can be seen from the simulation results that the main axis moves smoothly with a position error of about 0.01 arcsec, which is much better than the optimal 0.05 arcsec of the other control strategies that we simulated at an earlier time.

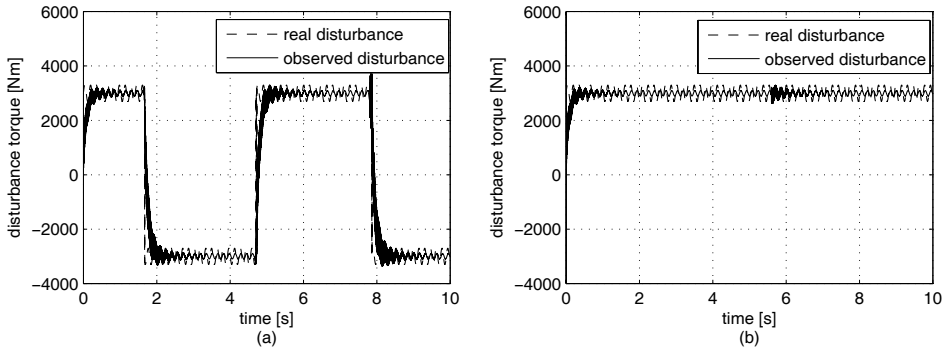

Fig. 3 (a) Observed disturbance vs. real disturbance when position tracking a sine wave reference. (b) Observed disturbance vs. real disturbance when position tracking a slope reference.

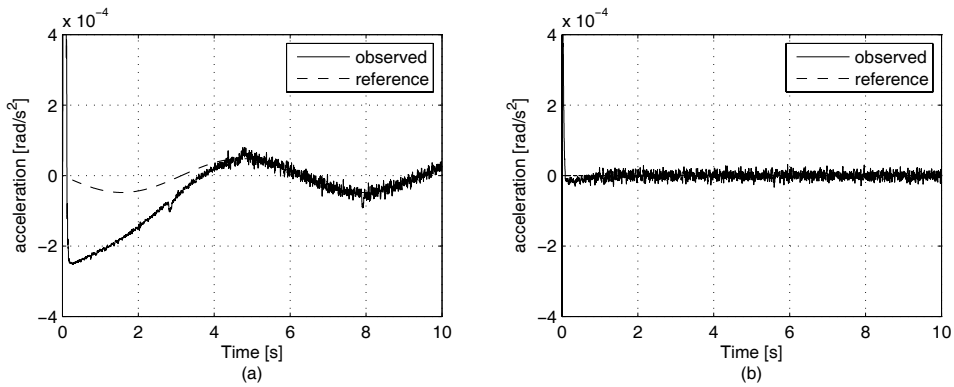

Fig. 4 (a) Observed acceleration signal vs. a sine wave reference. (b) Observed acceleration signal vs. a slope reference.

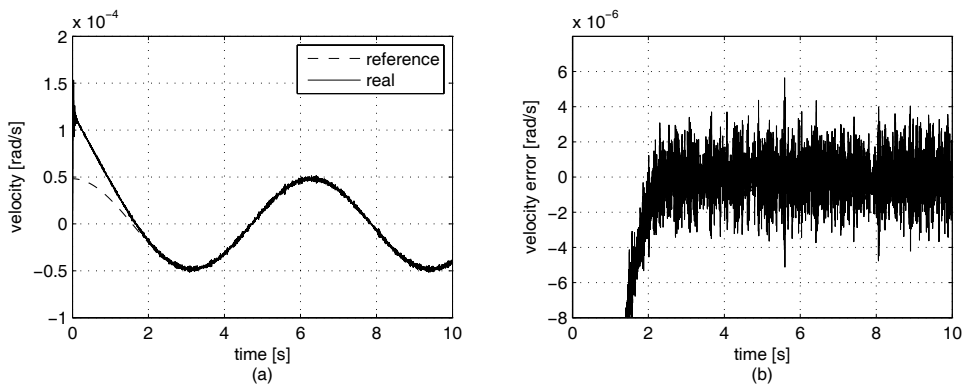

Fig. 5 (a) Velocity tracking of a sine wave reference. (b) Velocity tracking error.

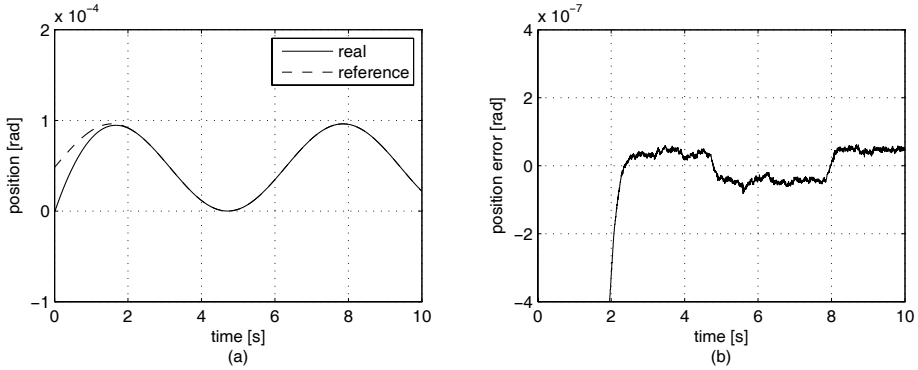

Fig. 6 (a) Position tracking of a sine wave reference. (b) Position tracking error.

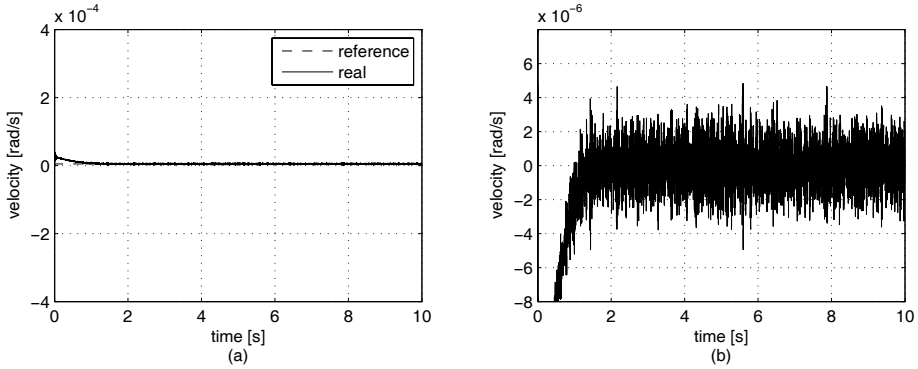

Fig. 7 (a) Velocity tracking of a slope reference. (b) Velocity tracking error.

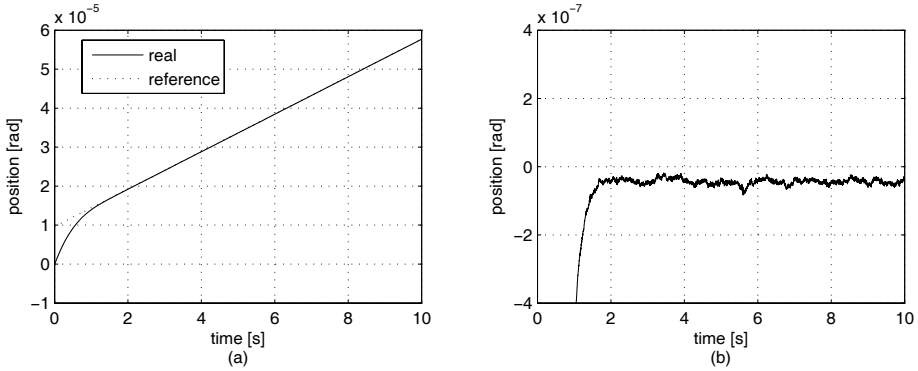

Fig. 8 (a) Position tracking of a slope reference. (b) Position tracking error.

Figures 7 and 8 show the tracking performances of the given approach with a slope reference. They also reveal nice tracking results where chattering phenomena are totally removed. The position error is restricted to less than 0.01 arcsec in the same way. It is not surprising that there are rather large velocity tracking errors in both cases because some noise is added to the measured velocity signals.

6 CONCLUSIONS

Due to the giant moment of inertia, nonlinear external wind disturbances and uncertainties in the system, it is difficult to control the main axes of the drive system of LAMOST when it runs at an ultra-low velocity. Though the general sliding mode may meet the position tracking requirements, it usually leads to a chattering phenomenon which can easily attain higher order terms or even result in instability. When properly designed, the higher order sliding mode can totally eliminate the chattering while requiring all system states to be available. Hence, a nonlinear adaptive observer is designed to obtain the acceleration signal for a third order sliding mode controller which could be used in the drive system of LAMOST. Simulations are done in Matlab which show excellent tracking performances that satisfy the demands.

Acknowledgements We would like to thank Prof. X. Q. Xu for his important suggestions, and we also thank Dr. B. R. Xie for her kind and warm help in English improvement. This work was funded by the National Natural Science Foundation of China (Grant No. 10903003), and the foundation of Nanjing University of Information Science & Technology (No. 20080309).

References

Bartolini, G., Pisano, A., Punta, E., & Usai, E. 2003, International Journal of Control, 76, 875
Burns, M. K. 1994, Proceeding of SPIE, 2199, 805
Canudas, De Wit C. 1998, IEEE Trans. Automatic Control, 43, 1189
Davenport, A. G. 1995, Journal of Wind Engineering and Industrial Aerodynamics, 54/55, 657
Dupont, P. E. 1994, IEEE Trans. Automatic Control, 39, 1094
Erm, T., Hurak, Z., & Bauvir, B. 2004, Proceeding of SPIE, 5496, 68
Feng, C.-B., & Fei, S.-M. 1998, Analysis and Design of Nonlinear Control System (Beijing: Publishing House of Electronics Industry)
Furuta, K., & Pan, Y. 2000, Automatica, 36, 211
Hirvonen, M., Pyrhonen, O., & Handroos, H. 2006, Mechatronics, 16, 279
Levant, A. 1998, Proc. of the 6th IEEE Mediterranean Conference on Control and Systems, June 9-11, Alghero, Sardinia, Italy
Levant, A. 2003, International Journal of Control, 76, 924
Marino, R., & Tomei, P. 2006, Nonlinear Control Design: Geometric, Adaptive and Robust (Beijing: Publishing House of Electronics Industry)
Medrano-Cerda, G., Lett, R., & Rees, P. 2002, Proceeding of SPIE, 4836, 88
Perruquetti, W., & Barbot, J. 2002, Sliding Mode Control in Engineering (NewYork: Marcel Dekker Inc. Press)
Sirota, M. J., Thompson, P. M., & Jex, H. R. 1994, Proceeding of SPIE, 2199, 126
Xu, X.-Q. 2000, Acta Astrophysica Sinica, 20, 43
Xu, X.-Q., & Yan, C.-H. 2004, Proceeding of SPIE, 5489, 1210
Zhou, W.-P., & Xu, X.-Q. 2008, Journal of System Simulation, 20, 3487
Zhou, W.-P., Xu, X.-Q., & Dong, Z.-M. 2006, Proceeding of SPIE, 6273(333), 1